Grey level co-occurrence matrix and its application to seismic data

Christoph Georg Eichkitz[1*], John Davies[2], Johannes Amtmann[1], Marcellus Gregor Schreilechner[1] and Paul de Groot[3] demonstrate how grey level co-occurrence matrix can be adapted to work on 3D imaging of seismic data.

Texture analysis is the extraction of textural features from images (Tuceryan and Jain, 1998). The meaning of texture varies, depending on the area of science in which it is used. In general, texture refers to the physical character of an object or the appearance of an image. In image analysis, texture is defined as a function of the spatial variation in intensities of pixels (Tuceryan and Jain, 1998). Seismic texture refers to the magnitude and variability of neighbouring amplitudes at sample locations and is physically related to the distribution of scattering objects (geological texture) within a small volume at the corresponding subsurface location (Gao, 2008). Four principal methods have been developed for the analysis of seismic texture (Figure 1). These are texture classification, segmentation, synthesis, and shape.

The aim of texture classification is to categorize features in an image by recognizing known texture classes. This approach is easy to compute and is the most used method of texture analysis. Texture segmentation partitions an image into different regions that have homogeneous properties. The segmentation can be either based on regions or based on boundaries between regions. In texture synthesis, small sample images are used as the basis for the construction or reconstruction of larger images. This methodology is widely applied in the reconstruction of digital images and in post-production of films. Texture shape is the least used method of texture analysis. It uses texture information to construct 3D surface geometries.

According to Tuceryan and Jain (1998), texture classification can be divided into four computational categories: statistical, geometrical, model-based, and signal processing methods of computation. Numerous applications are available that employ each of these methods.

Statistical texture analysis, such as the grey level co-occurrence matrix (GLCM), grey level differences, or local binary pattern extraction, try to define the arrangement of different regions in an image through statistics. Statistical methods do not attempt to understand the hierarchical

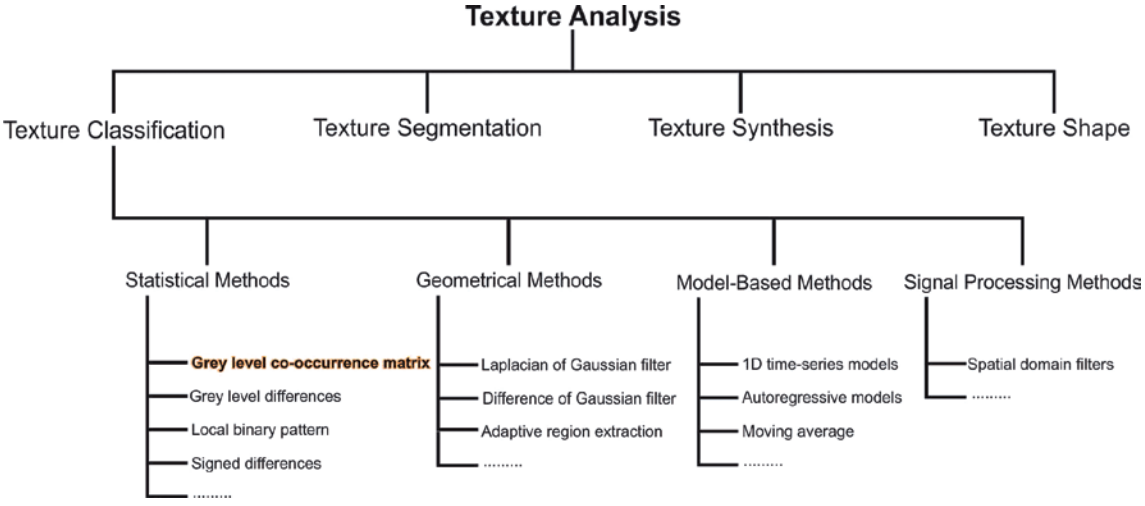

Figure 1 *Texture analysis includes texture classification, texture segmentation, texture synthesis, and texture shape. Texture classification can be divided into four categories of computation: statistical methods, geometrical methods, model-based methods, and signal processing methods.*

[1] *Joanneum Research, Institute for Water, Energy and Sustainability, Group of Geophysics and Geothermics, Leoben, Austria.*
[2] *Heinemann Oil GmbH, Leoben, Austria.*
[3] *dGB Earth Sciences BV, Nijverheidstraat 11-2, 7511 JM Enschede, Netherlands.*
[*] *Corresponding Author, E-mail: christoph.eichkitz@joanneum.at*

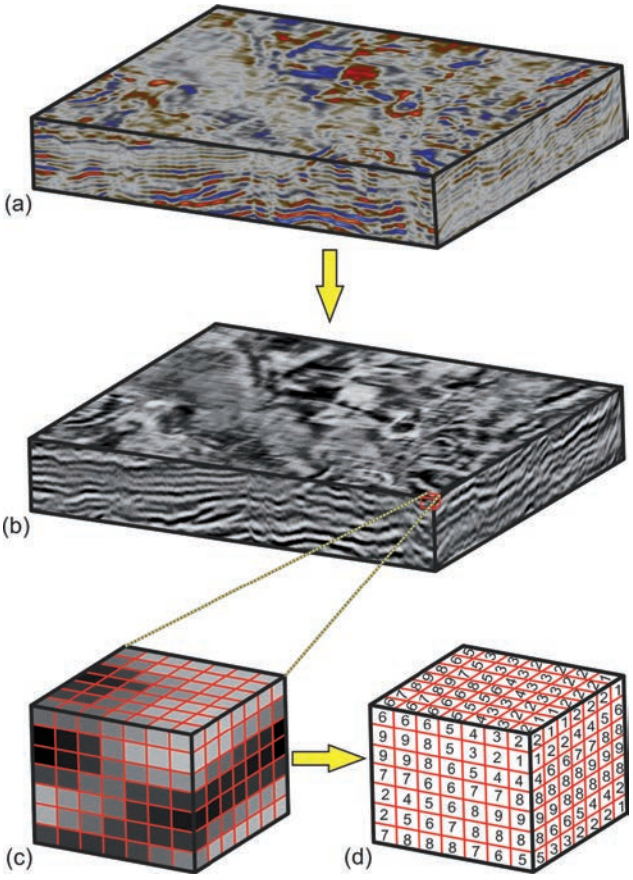

Figure 2 *Conversion of the seismic amplitude cube (a) in to grey level cube (b). The grey levels (c) are represented by discrete numbers (d).*

nature of a texture, but rather represent texture indirectly by non-deterministic properties that govern the distributions and relationships between samples of an image (Materka and Strzelecki, 1998). Geometrical texture analysis methods define texture as composed of well-defined textural elements or primitives (microtexture) and a hierarchy of spatial arrangements (macrotexture) of these primitives (Materka and Strzelecki, 1998). Geometrical texture analysis can be useful for symbolic description of images, but is more useful for synthesis than for analysis. Model-based texture analysis tries to describe texture by constructing image models. Model parameters are especially important, as they must capture the essential qualities of images. Signal processing methods usually apply a transformation to the data. This transformation is often based on a Fourier transform (Rosenfeld and Weszka, 1976), a Gabor transform (Daugman, 1985; Bovik et al., 1990), or a wavelet transform (Mallat, 1989; Laine and Fan, 1993; Lu et al., 1997).

Grey level co-occurrence matrix

The grey level co-occurrence matrix (GLCM) and its derived attributes are tools for image classification that were initially described by Haralick et al. (1973). The GLCM is a measure of how often different combinations of pixel brightness values occur in an image. Because typically two samples are compared, GLCM is referred to as a second order texture classification method. It is widely used for classification of satellite images (e.g. Franklin et al., 2001; Tsai et al., 2007), sea-ice images (e.g. Soh and Tsatsoulis, 1999; Maillard et al., 2005), magnetic resonance and computed tomography images (e.g. Kovalev et al., 2001; Zizzari et al., 2011), and in many other applications. Most of these GLCM applications involve classification of 2D images.

To apply GLCM to seismic data, the methods must be adapted to work on 3D data. Numerous investigators have devised solutions to this problem (e.g. Vinther et al., 1996; Gao, 1999, 2003, 2007, 2008a, 2008b, 2009, 2011; West et al., 2002; Chopra and Alexeev, 2005, 2006a, 2006b; Yenugu et al., 2010; de Matos et al., 2011). The methods by West et al. (2002) and Gao (2003, 2007, 2011) utilize flattened seismic cubes and the GLCM calculation is done on 2D planes

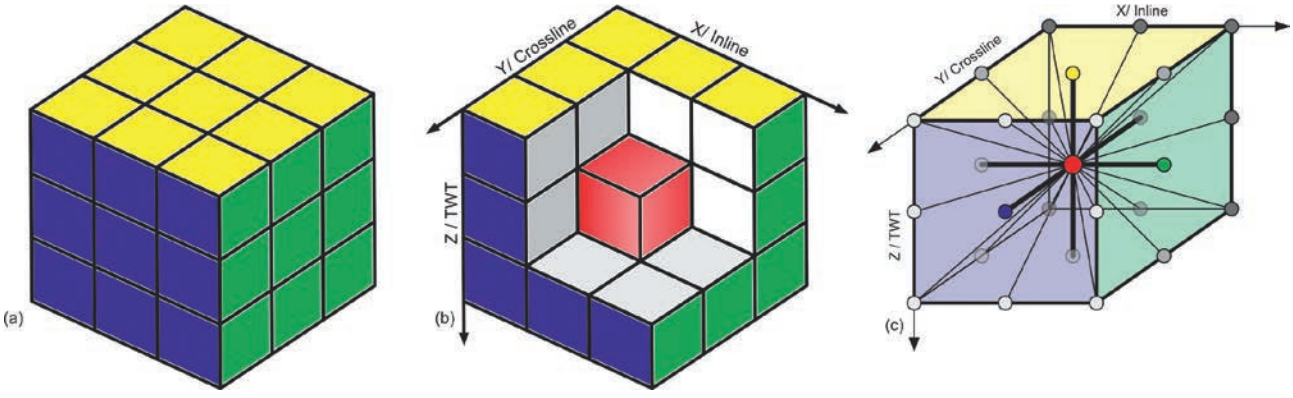

Figure 3 *In a 3D case the number of neighbors for one sample point can be best explained by examining a Rubik's cube (a). The center of the Rubik's cube (red box in (b)) has in total 26 neighboring boxes. The boxes are aligned in 13 directions. Analogous to this, a sample point in a seismic volume has 26 neighbours aligned in 13 directions (c).*

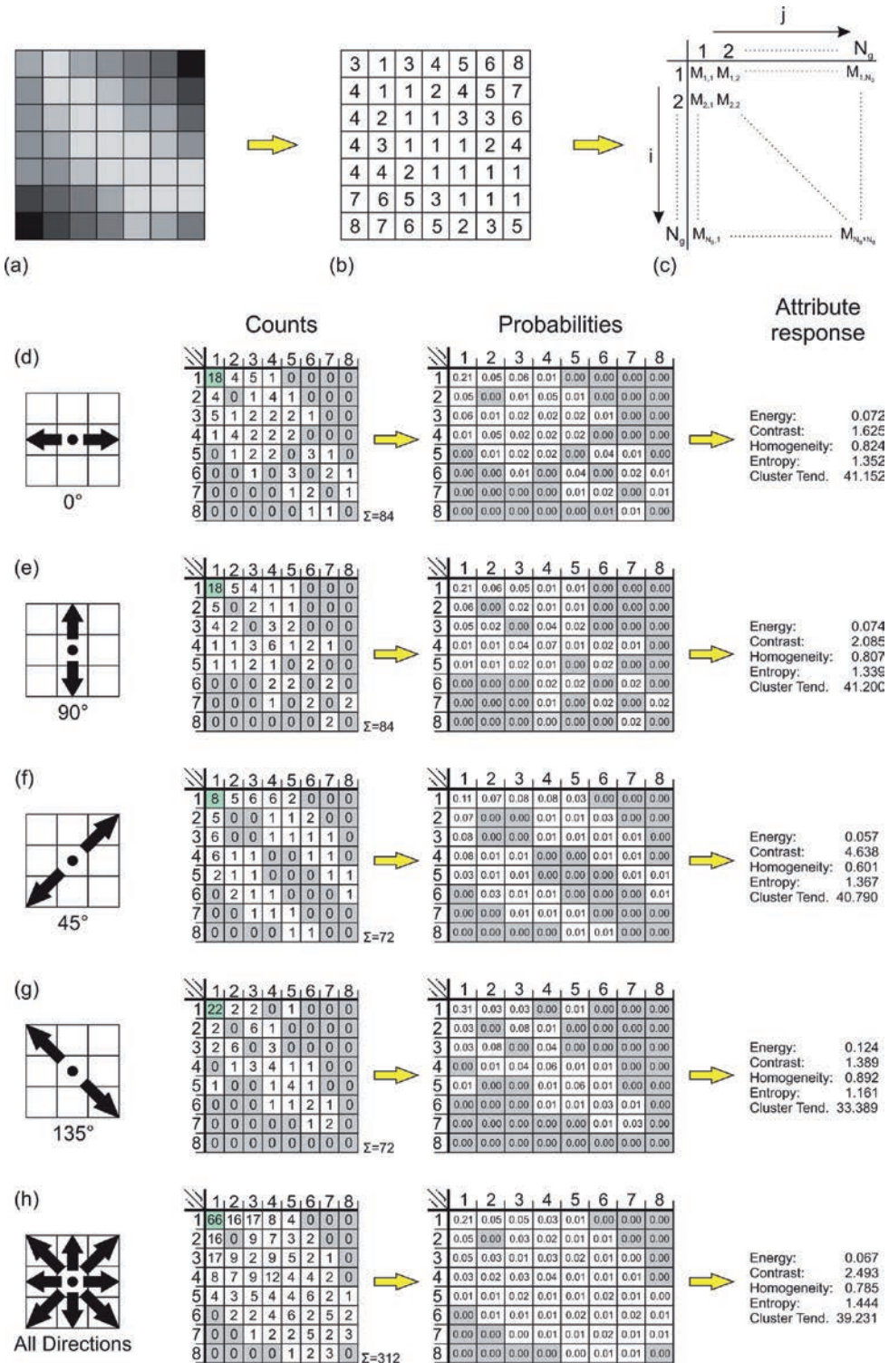

Figure 4 *Calculation of grey level co-occurrence matrix-based attributes using eight grey levels for a randomly generated 2D grey-scale image (a). Grey tones of the image can be represented by discrete values (b). Number of co-occurrences of pixel pairs for a given search window are counted and grey level co-occurrence matrix (c) is produced. Based on this co-occurrence matrix, grey level co-occurrence matrices are determined for horizontal (d), vertical (e), 45° diagonal (f), 135° diagonal (g), and for all directions simultaneously (h). Initial step in calculation is determination of co-occurrences (column 2). Zero entries are marked in light grey and the highest value of each matrix is marked in dark grey. Calculations in single directions lead to sparse matrices. The GLCM is normalized by the sum of all elements to yield a probability matrix (column 3). Probabilities are used to calculate GLCM-based attributes. Column 4 shows Entropy, Contrast, Homogeneity, Entropy, and Cluster Tendency.*

along the three coordinate axes. In a recent paper on GLCM applied to seismic data, de Matos et al. (2011) use a different approach. They calculate 2D GLCM along the structural dip and azimuth of the seismic cube, and in this manner they generate a pseudo 3D GLCM cube. Based on work by Tsai et al. (2007) and Lai et al. (2008) for 3D GLCM calculations on hyperspectral satellite data, a full 3D GLCM algorithm has been developed for seismic data (Eichkitz and Amtmann et al., 2012b, 2012c, 2013, 2014a, 2014b; Eichkitz and de Groot et al., 2014; Eichkitz et al., 2015).

Workflow for full 3D GLCM calculations

The first step in GLCM calculation is to transform the seismic input cube into a grey level cube in which each sample point is assigned a discrete number. A histogram of amplitude values in the seismic cube is generated and positive and negative thresholds are selected. The resulting amplitude range is divided into equal segments; the number of segments is equal to the desired number of grey levels (Figure 2). For seismic data this value typically is between 4 Bits (16 grey levels) and 8 Bits (256 grey levels).

The GLCM calculation is done using a running window. From each sample in the data, a subset is extracted and within this subset all sample combinations are measured and written into a 2D matrix. The extracted subset is defined by an analysis window (for 2D data) or by an analysis cube (for 3D data). In both cases, the sample point of interest is at the centre of the subset and the analysis window or cube consists of odd numbers of sample points in all directions. The measurement of sample co-occurrences can be done in several directions. For 2D data, four space directions are possible and for 3D data, 13 space directions are possible with an offset of 1(Figure 3). It is possible to measure co-occurrences in a single direction and obtain textural information in that specific direction. The process can be repeatedly applied to determine textural measures for all other directions. Alternatively, co-occurrences can be calculated simultaneously in multiple directions, producing a generalized measurement of texture for the whole structure. Analyses using this approach give smoother results, but subtle information may be lost. The number of co-occurrences between all pairs of samples is entered in a symmetrical 2D matrix of the same size as the number of grey levels in the image. For further calculation of GLCM-based attributes, normalization of this matrix is necessary. All matrix entries are divided by the total number of co-occurrences, producing a matrix of proportions that can be regarded as a kind

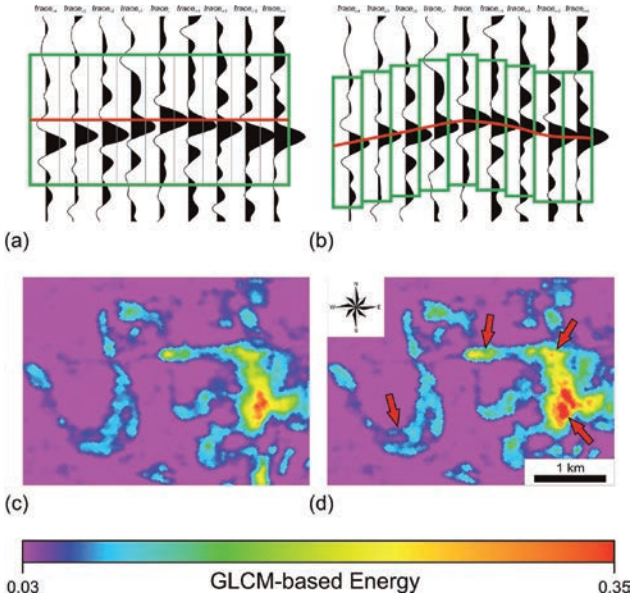

Figure 5 *Structural dip is computed by complex trace analysis, discrete scan, or gradient structure tensor approach. Here, a discrete scan produced the best results. Images (a and c) represent calculation without using structural dip. Vertical positions of peak amplitudes are not aligned horizontally in (a and b). If structural dip is neglected, the centre of the analysis window falls at the red line (a) and the analysis window is a perfect cube. (c) GLCM-based energy in 0° direction without dip guidance. (d) GLCM-based energy in 0° direction with dip guidance. In dip-guided computation the signal to noise ratio is higher and certain features can be better imaged (red arrows).*

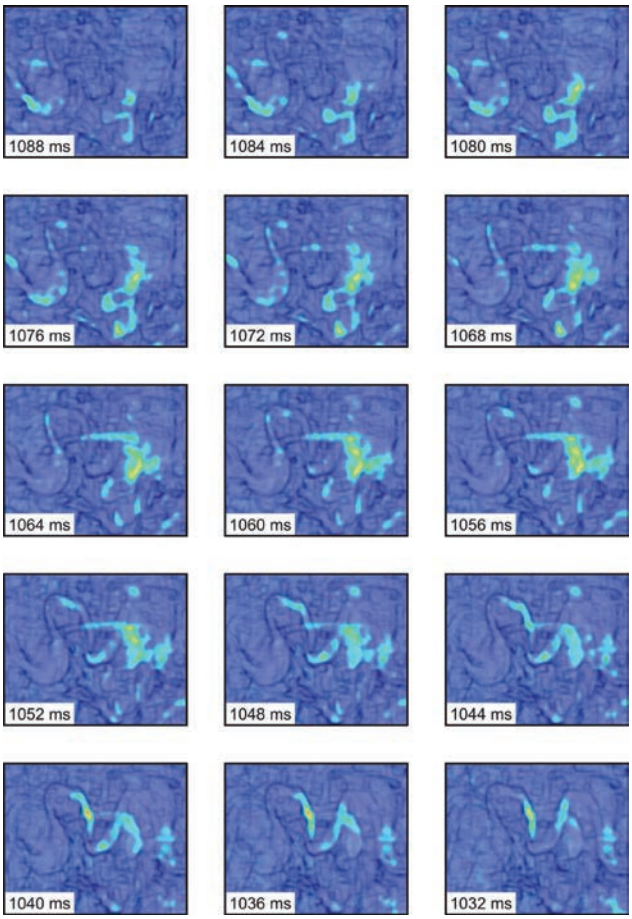

Figure 6 *GLCM-based energy time-slice with superimposed coherence attribute. GLCM-based energy shows areas within the channel system, whereas coherence attribute shows channel edges.*

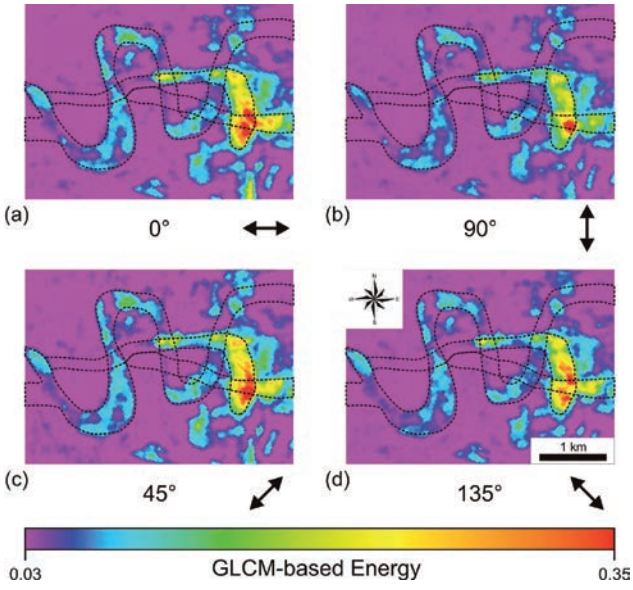

Figure 7 *GLCM-based energy attribute calculated in four different space directions. (a) 0 direction (east-west), (b) 90° direction (north-south), (c) 45° direction (northeast-southwest), (d) the 135° direction (northwest-southeast).*

of probability matrix. Haralick et al. (1973) proposed 14 attributes based on this probability matrix. Soh and Tsatsoulis (1999) and Wang et al. (2010) developed ten additional attributes based on the GLCM. The calculated GLCM-based attributes are assigned to the centre point of the analysis window. This procedure is repeated for all sample points within the seismic data cube (Figure 4). Figure 2 shows a two-dimensional synthetic image to illustrate the steps in GLCM-based attribute calculations.

For other attribute calculations the integration of dip guidance is very important. By integrating the volumetric dip, the input volume is warped along the seismic stratigraphy (Figure 5a and 5b) so the analysis window is no longer a rectangular cube. Integration of dip guidance results in much sharper images that are easier to interpret as signals from different seismic reflectors are not mixed. Integration of dip guidance also affects the range of values of the resulting attributes. Dip-guided GLCM attributes tend to have a wider range than attributes that are not dip guided (Figure 5c and 5d).

Fields of application

The main application of GLCM is for seismic facies description. West et al. (2002) used GLCM-based attributes in combination with neural networks to describe details of channel facies. This information was then used to estimate net-to-gross ratios within interpreted channel structures. Gao (2007) and Angelo et al. (2011) also used GLCM to describe channel structures and the distribution of facies within these channels. We applied the GLCM method to a seismic survey from the Vienna Basin to describe a Middle

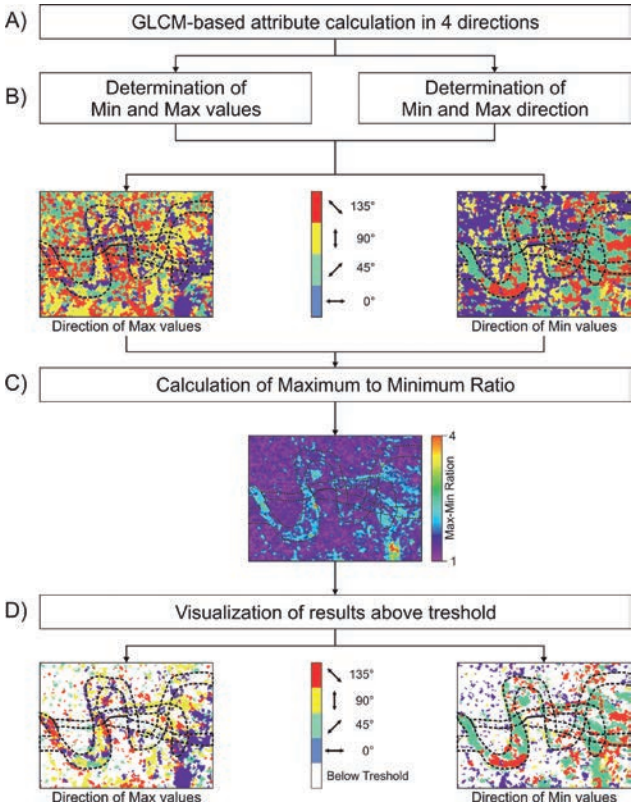

Figure 8 *Workflow for seismic amplitude variability detection using GLCM-based attributes: (A) Calculation of each GLCM-based attribute in four space directions (only four horizontal directions are shown). (B) Determination of minima and maxima values and their direction for each GLCM-based attribute. (C) Calculation of ratio between maximum and minimum, used to determine threshold value. (D) Application of threshold value to identify areas with higher directional variability and visualize only directions of minima and maxima.*

to Upper Miocene (Sarmatian or Pannonian age) channel system that has an average width of 130-300 m (426-984 ft) and an average thickness of 70 ms. Channel edges can easily be interpreted using coherence attributes, but these fail to give information about the channel interior. By using GLCM attributes the channel appears as a body of more or less uniform colours that strongly contrast with the surrounding facies (Figure 6).

Detection of directional variability

Anisotropy describes the directional dependencies of any property. Seismic anisotropy is the dependence of velocity on direction or upon angle (e.g., Crampin 1981, 1985; Lynn and Thomsen, 1990; Willis et al., 1986, Martin and Davis, 1987; Thomsen, 1986; Alkhalifah and Tsvankin, 1995). Seismic anisotropy can be caused by spatial variation in sediments, the presence of fractures and fault zones, and by differences in pore fillings. The description of fractured zones is especially important for hydrocarbon exploration. In Figure 5, a GLCM-based energy attribute calculated in four

horizontal directions is shown. In the four images there are small variations in amplitude values, but all images appear more or less the same and it is nearly impossible to perceive any anisotropy. We have developed an automatic workflow (Figure 6) to distinguish between areas with a high degree of anisotropy from areas of low anisotropy (Eichkitz et al., 2015). In this workflow attribute responses from directional GLCM-based attributes are compared. An attribute set is calculated based on these comparisons, providing information about directional behaviour. The exact same attribute response is rarely obtained for all directions. In some areas, the minimum and maximum values may be very similar and lead to an overestimation of anisotropy. To overcome this problem it is necessary to condition the output from step (B) to distinguish between areas having high directional variability from areas with low directional variability. In step (C) of the workflow, a ratio cube between maximum and minimum values for each GLCM-based attribute is calculated and a threshold value is manually determined. The threshold value is then used in step (D) to set all areas having a ratio below the threshold to no directional variability. In other words, areas with ratio values below the threshold are assigned an undefined anisotropy value, whereas the other areas are assigned the corresponding minimum, maximum, direction of minimum, and direction of maximum values.

A single GLCM-based attribute is not sufficient for detailed interpretations of seismic anisotropy. It is necessary to compute several GLCM-based attributes and combine these to form a comprehensive interpretation. It is then possible to determine areas that have greater directional variability, possibly caused by fracturing or related to changes in lithology or pore filling. Directional information from this analysis may help to determine fracture strike and dip.

Conclusion

Although texture attributes have not been used widely in seismic interpretation, GLCM can provide important insight into the subsurface through attribute analysis. Different authors have shown that the GLCM is a useful tool for the description of seismic facies. Because GLCM-based attributes can be calculated in different directions, they can be used to determine directional variations in seismic data. This opens the door to differentiate between sedimentary facies and patterns of fracturing, including the delineation of fractured zones and their strike and dip.

Acknowledgements

We would like to thank OMV for providing data sets, funding this research project, and for permission to publish this paper.

References

Alkhalifah, T. and Tsvankin, I. [1995] Velocity analysis for transversely isotropic media. *Geophysics*, **60** (5), 1550-1566.

Angelo, S.M., de Matos, M. and Marfurt, K.J. [2009] Integrated seismic texture segmentation and clustering analysis to improved delineation of reservoir geometry. *79th SEG meeting*, Expanded Abstracts.

Bovik, A.C., Clark, M. and Geisler, W.S. [1990] Multichannel texture analysis using localized spatial filters. *Pattern Analysis and Machine Intelligence*, **12** (1), 55-73.

Chopra, S., and Alexeev, V. [2005] Application of texture attribute analysis to 3D seismic data. *75th SEG meeting*, Expanded Abstracts, 767-770.

Chopra, S. and Alexeev, V. [2006a] Application of texture attribute analysis to 3D seismic data. *The Leading Edge*, **25** (8), 934-940.

Chopra S. and Alexeev, V. [2006b] Texture attribute application to 3D seismic data. *6th International Conference & Exposition on Petroleum Geophysics*, Expanded Abstracts, 874-879.

Crampin, S. [1981] A review of wave motion in anisotropic and racked elastic-media. *Wave Motion*, **3** (4), 343-391.

Crampin, S. [1985] Evaluation of anisotropy by shear-wave splitting. *Geophysics*, **50** (1), 142-152.

Daugman, J.G. [1985] Uncertainty relation for resolution in space, spatial frequency, and orientation optimized by two-dimensional visual cortical filters. *Journal of the Optical Society of America*, **2** (7), 1160-1169.

De Matos, M.C., Yenugu, M., Angelo, S.M. and Marfurt, K.J. [2011] Integrated seismic texture segmentation and cluster analysis applied to channel delineation and chart reservoir characterization. *Geophysics*, **76** (5), P11-P21.

Eichkitz, C.G., Amtmann, J. and Schreilechner, M.G. [2012a] Enhanced coherence attribute imaging by structural oriented filtering. *First Break*, **30** (3), 75-81.

Eichkitz, C.G., Amtmann, J. and Schreilechner, M.G. [2012b] Facies Characterization by Seismic Texture Analysis Using Grey Level Co-occurrence Matrix Based Attributes. *74th EAGE Conference & Exhibition*, Extended Abstracts.

Eichkitz, C.G., Amtmann, J. and Schreilechner, M.G. [2013] Calculation of grey level co-occurrence matrix-based seismic attributes in three dimensions. *Computers and Geosciences*, **60**, 176-183.

Eichkitz, C.G., Amtmann, J. and Schreilechner, M.G. [2014a] Application of GLCM-based seismic attributes for anisotropy detection. *76th EAGE Conference & Exhibition*, Extended Abstracts.

Eichkitz, C.G., de Groot, P. and Brouwer, F. [2014] Visualizing anisotropy in seismic facies using stratigraphically constrained, multi-directional texture attribute analysis. *AAPG Hedberg Research Conference "Interpretation Visualization in the Petroleum Industry"*, Houston, USA.

Eichkitz, C.G., Schreilechner, M.G., de Groot, P. and Amtmann, J. [2015] Mapping directional variations in seismic character using GLCM-based attributes. *Interpretation*, **3** (1), T13-T23.

Franklin, S.E., Maudie, A.J. and Lavigne, M.B. [2001] Using spatial co-occurrence texture to increase forest structure and species composition classification accuracy. *Photogrammetric Engineering & Remote Sensing*, **67** (7), 849-855.

Gao, D. [2011] Latest developments in seismic texture analysis for subsurface structure, facies, and reservoir characterization: A review. *Geophysics*, **76** (2), W1-W13.

Gao, D. [2009] 3D seismic volume visualization and interpretation: An integrated workflow with case studies. *Geophysics*, **74** (1), W1-W24.

Gao, D. [2008a] Adaptive seismic texture model regression for subsurface characterization. *Oil & Gas Review*, **6** (11), 83-86.

Gao, D. [2008b] Application of seismic texture model regression to seismic facies characterization and interpretation. *The Leading Edge*, **27** (3), 394-397.

Gao, D. [2007] Application of three-dimensional seismic texture analysis with special reference to deep-marine facies discrimination and interpretation: Offshore Angola, West Africa. *AAPG Bulletin*, **91** (12), 1665-1683.

Gao, D. [2003] Volume texture extraction for 3D seismic visualization and interpretation. *Geophysics*, **68** (4), 1294-1302.

Gao, D. [1999] 3D VCM seismic textures: A new technology to quantify seismic interpretation. *69th SEG meeting*, Expanded Abstracts, 1037-1039.

Haralick, R.M., Shanmugam, K. and Dinstein, I. [1973] Textural features for image classification. *IEEE Transactions on systems, man, and cybernetics*, **3** (6), 610-621.

Kovalev, V.A., Kruggel, F., Gertz, H.-J. and von Cramon, D.Y. [2001] Three-dimensional texture analysis of MRI brain datasets. *IEEE Transactions on medical imaging*, **20** (5), 424-433.

Lai, J.-S. and Tsai, F. [2008] Three dimensional texture computation of gray level co-occurrence tensor in hyperspectral image cubes. *Proc. 29th Asian Conference on Remote Sensing (ACRS2008)*, Colombo, Sri Lanka.

Laine, A. and Fan, J. [1993] Texture classification by wavelet packet signatures. *Pattern Analysis and Machine Intelligence*, **15** (11), 1186-1191.

Lu, C.S., Chung, P.C. and Chen, C.F. [1997] Unsupervised texture segmentation via wavelet transform. *Pattern Recognition*, **30** (5), 729-742.

Lynn, H.B. and Thomsen, L.A. [1990] Reflection shear-wave data collected near the principal axes of azimuthal anisotropy. *Geophysics*, **55** (2), 147-156.

Maillard, P., Clausi, D.A. and Deng, H. [2005] Operational map-guided classification of SAR sea ice imagery. *IEEE Transaction on Geoscience and Remote Sensing*, **43** (12), 2940-2951.

Mallat, S.G. [1989] A theory for multiresolution signal decomposition: the wavelet representation. *Pattern Analysis and Machine Intelligence*, **11** (7), 674-693.

Martin, M.A. and Davis, T.L. [1987] Shear-wave birefringence: A new tool for evaluating fractured reservoirs. *The Leading Edge*, **6** (10), 22-28.

Materka, A. and Strzelecki, M. [1998] *Texture analysis methods – a review*. Technical University of Lodz, Institute of Electronics, 33.

Rosenfeld, A. and Weszka, J.S. [1976] Picture recognition and scene analysis. *Computer*, **9** (5), 28-38.

Soh, L.-K. and C. Tsatsoulis [1999] Texture analysis of SAR sea ice imagery using gray level co-occurrence matrices. *IEEE Transactions on Geoscience and Remote Sensing*, **37** (2), 780-795.

Thomsen, L. [1986] Weak elastic anisotropy. *Geophysics*, **51** (10), 1654-1966.

Tsai, F., Chang, C.-T., Rau, J.-Y., Lin, T.-H. and Liu, G.-R. [2007], 3D computation of gray level co-occurrence in hyperspectral image cubes. *LNCS 4679*, 429-440.

Tuceryan, M. and Jain, A.K. [1998] *Texture analysis. The handbook of pattern recognition and computer vision.*

Vinther, R., Mosegaar, K., Kierkegaard, K., Abatzi, I., Andersen, C., Vejbaek, O.V., If, F. and Nielsen, P.H. [1996] Seismic texture classification: A computer-aided approach to stratigraphic analysis. *65th SEG meeting*, Houston, Texas, USA, 153-155.

Wang, H., Guo, X.-H., Jia, Z.-W., Li, H.-K., Liang, Z.-G., Li, K.-C. and He, Q. [2010] Multilevel binomial logistic prediction model for malignant pulmonary nodules based on texture features of CT image. *European Journal of Radiology*, **74**, 124-129.

West, B.P., May, S.R., Eastwood, J.E. and Rossen, C. [2002] Interactive seismic facies classification using textural attributes and neural networks. *The Leading Edge*, **21** (10), 1042-1049.

Willis, H., Rethford, G. and Bielanski, E. [1986] Azimuthal anisotropy: Occurrence and effect on shear wave data quality. *56th SEG Annual International Meeting*, Expanded Abstracts.

Yenugu, M., Marfurt, K.J. and Matson, S. [2010] Seismic texture analysis for reservoir prediction and characterization. *The Leading Edge*, **29** (9), 1116-11.

Zizzari, A., Seiffert, U., Michaelis, B., Gademann, G. and Swiderski, S. [2001] Detection of tumor in digital images of the brain. *Proc. of the IASTED international conference Signal Processing, Pattern Recognition & Applications*, Rhodes, Greece, 132-137.